A Novel Radon-Wavelet Based OFDM System Design and Performance Under Different Channel Conditions

Abbas Kattoush
EE Engineering Department, Tafila Technical University, Jordan

Abstract: *Finite Radon Transform mapper has the ability to increase orthogonality of sub-carriers, it is non sensitive to channel parameters variations, and has a small constellation energy compared with conventional Fast Fourier Transform based orthogonal frequency division multiplexing. It is also able to work as a good interleaver which significantly reduces the bit error rate. Due to its good orthogonality, discrete wavelet transform is used for orthogonal frequency division multiplexing systems which reduces inter symbol interference and inter carrier interference. This eliminates the need for cyclic prefix and increases the spectral efficiency of the design. In this paper both Finite Radon Transform and Discrete Wavelet Transform are implemented in a new design for orthogonal frequency division multiplexing. The new structure was tested and compared with conventional Fast Fourier Transform -based orthogonal frequency division multiplexing, Radon-based orthogonal frequency division multiplexing, and discrete wavelet transform -based orthogonal frequency division multiplexing for additive white Gaussian noise channel, flat fading channel, and multi-path selective fading channel. Simulation tests were generated for different channels parameters values. The obtained results showed that proposed system has increased spectral efficiency, reduced inter symbol interference and inter carrier interference, and improved bit error rate performance compared with other systems.*

Keywords: *Discrete Wavelet Transform, Finite Radon Transform, radon based OFDM, DWT based OFDM, and OFDM.*

Received April 8, 2009; accepted August 4, 2009

1. Introduction

Orthogonal frequency division multiplexing system is one of the most promising technologies for current and future wireless communications. It is a form of multi-carrier modulation technologies where data bits are encoded to multiple sub-carriers, while being sent simultaneously [1]. Each sub-carrier in an Orthogonal Frequency Division Multiplexing (OFDM) system is modulated in amplitude and phase by the data bits. Modulation techniques typically used are binary phase shift keying, Quadrature Phase Shift Keying (QPSK), Quadrature Amplitude Modulation (QAM), 16-QAM, 64-QAM etc., The process of combining different sub-carriers to form a composite time-domain signal is achieved using Fast Fourier Transform (FFT) and Inverse FFT (IFFT) operations [25].

The main problem in the design of a communications system over a wireless link is to deal with multi-path fading, which causes a significant degradation in terms of both the reliability of the link and the data rate [20]. Multi-path fading channels have a severe effect on the performance of wireless communication systems even those systems that exhibits efficient bandwidth, like OFDM [12]. There is always a need for developments in the realization of these systems as well as efficient channel estimation and equalization methods to enable these systems to reach their maximum performance [26]. The OFDM receiver structure allows relatively straightforward signal processing to combat channel delay spreads, which was a prime motivation to use OFDM modulation methods in several standards [11, 13, 19, 21].

In transmissions over a radio channel, the orthogonality of the signals is maintained only if the channel is flat and time-invariant, channels with a Doppler spread and the corresponding time variations corrupt the orthogonality of the OFDM sub-carrier waveforms [6]. In a dispersive channel, self-interference occurs among successive symbols at the same sub-carrier casing Inter Symbol Interference (ISI), as well as among signals at different sub-carriers casing Inter Carrier Interference (ICI). For a time-invariant but frequency-selective channel, ICI, as well as ISI, can effectively be avoided by inserting a cyclic prefix before each block of parallel data symbols at the cost of power loss and bandwidth expansion [25].

The Radon Transform (RT) was first introduced by Johann Radon (1917) and the theory, basic aspects, and applications of this transform are studied in [4, 7] while the Finite RAdon Transform (FRAT) was first studied by [3]. RT is the underlying fundamental concept used for computerized tomography scanning, as well for a wide range of other disciplines, including radar imaging, geophysical imaging, nondestructive testing and medical imaging [11]. Recently FRAT was proposed as a mapping technique in OFDM system [2]. Conventional OFDM/QAM systems are robust for multi-path channels due to the cyclically prefixed guard interval which is inserted between consequent symbols to cancel ISI. However, this guard interval decreases the spectral efficiency of the OFDM system as the corresponding amount [24]. Thus, there have been approaches of wavelet-based OFDM which does not require the use of the guard interval [10, 14, 15, 23, 27, 28, 29]. It is found that OFDM based on Haar orthonormal wavelets (DWT-OFDM) are capable of reducing the ISI and ICI, which are caused by the loss in orthogonality between the carriers.

In this paper the idea of one dimensional serial Radon based OFDM proposed in [2] is developed farther towards increasing spectral efficiency and reducing BER. Further performance gains and higher spectral efficiency were made by combining both FRAT and DWT in the design of OFDM system. Simulation results show that proposed system has better performance than Fourier, Radon, and wavelet based OFDM under different channel conditions.

The paper is organized as follows. In section 2 we describe the serial one-dimensional OFDM system and provide the algorithm for computing the mapping data; in section 3 we describe and provide a fast discrete wavelet transform computation algorithm used in proposed system design; in section 4 we describe the proposed Radon-wavelet-OFDM system and in section 5 we provide the simulation analyze and discussions of the obtained results; Finally in section 6, a conclusion is presented to summarize the main outcomes of this paper.

2. The Radon-Based OFDM

Radon-based OFDM was recently proposed in [2], it was found that as a result of applying FRAT, the Bit Error Rate (BER) performance was improved significantly, especially in the existence of multi-path fading channels. Also, it is found that Radon-based OFDM structure is less sensitive to channel parameters variation, like maximum delay, path gain, and maximum Doppler shift in selective fading channels as compared with standard OFDM structure.

In Radon based OFDM system, FRAT mapping is used instead of QAM mapping [2] as shown in Figure 1. The other processing parts of the system remain the same as in conventional QAM OFDM system. It is known that FFT based OFDM obtain the required orthogonality between sub-carriers from the suitability of IFFT algorithm [12, 25, 26]. Using FRAT mapping with the OFDM structure increases the orthogonality between sub-carriers since FRAT computation uses one-Dimensional (1-D) IFFT algorithm. Also FRAT is designed to increase the spectral efficiency of the OFDM system through increasing the bit per Hertz of the mapping. Sub carriers are generated using N points Discrete Fourier Transform (DFT) and Guard Interval (GI) inserted at start of each symbol is used to reduce ISI.

The procedure steps of using the Radon based OFDM mapping is as follows:

Step 1: suppose $d(k)$ is the serial data stream to be transmitted using OFDM modulation scheme. Converting $d(k)$ from serial form to parallel form will construct a one dimensional vector containing the data symbols to be transmitted,

$$d(k) = (d_0\ d_1\ d_2 \ldots\ldots d_n)^T \tag{1}$$

where, k and n are the time index and the vector length respectively.

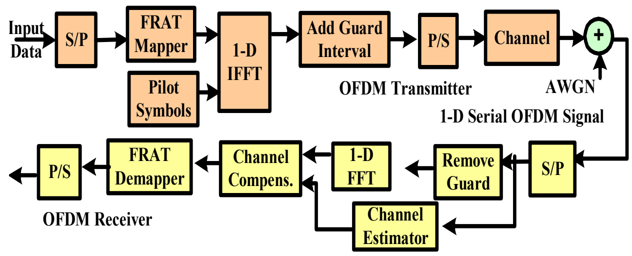

Figure 1. Serial Radon based OFDM transceiver.

Step 2: convert the data packet represented by the vector *d(k)* from one-dimensional vector to a *pxp* two dimensional matrix *D(K)*, where *p* should be a prime number according to the matrix resize operation.

Step 3: take the 2-D FFT of the matrix *D(K)* to obtain the matrix, *F(r, s)*. For simplicity it will be labeled by *F*.

$$F(r,s) = \sum_{m=0}^{p-1}\sum_{n=0}^{p-1} D(m,n) e^{-j(2\pi/p)rm} e^{-j(2\pi/p)ns} \tag{2}$$

Step 4: redistribute the elements of the matrix *F* according to the optimum ordering algorithm given in [17], so, the dimensions of the resultant matrix will be $p\times(p+1)$ and will be denoted by the symbol $\mathcal{F}_{opt}$. The two matrixes for FRAT window= 7 are given by:

$$\mathcal{F} = \begin{bmatrix} f_1 & f_8 & f_{15} & f_{22} & f_{29} & f_{36} & f_{43} \\ f_2 & f_9 & f_{16} & f_{23} & f_{30} & f_{37} & f_{44} \\ f_3 & f_{10} & f_{17} & f_{24} & f_{31} & f_{38} & f_{45} \\ f_4 & f_{11} & f_{18} & f_{25} & f_{32} & f_{39} & f_{46} \\ f_5 & f_{12} & f_{19} & f_{26} & f_{33} & f_{40} & f_{47} \\ f_6 & f_{13} & f_{20} & f_{27} & f_{34} & f_{41} & f_{48} \\ f_7 & f_{14} & f_{21} & f_{28} & f_{35} & f_{42} & f_{49} \end{bmatrix} \tag{3}$$

$$\mathcal{F}_{opt} = \begin{bmatrix} f_1 & f_1 & f_1 & f_1 & f_1 & f_1 & f_1 & f_1 \\ f_2 & f_{10} & f_9 & f_{16} & f_8 & f_{21} & f_{14} & f_{13} \\ f_3 & f_{19} & f_{17} & f_{31} & f_{15} & f_{34} & f_{20} & f_{18} \\ f_4 & f_{28} & f_{25} & f_{46} & f_{22} & f_{47} & f_{26} & f_{23} \\ f_5 & f_{30} & f_{33} & f_{12} & f_{29} & f_{11} & f_{32} & f_{35} \\ f_6 & f_{39} & f_{41} & f_{27} & f_{36} & f_{24} & f_{38} & f_{40} \\ f_7 & f_{48} & f_{49} & f_{42} & f_{43} & f_{37} & f_{44} & f_{45} \end{bmatrix} \tag{4}$$

Step 5: take the 1D-IFFT for each column of the matrix $\mathcal{F}_{opt}$ to obtain the matrix of Radon coefficients, R :

$$R = \frac{1}{p} \sum_{k=0}^{N-1} F_{opt}\, e^{\frac{j 2 \pi k n}{p}} \tag{5}$$

Step 6: construct the complex matrix $\overline{R}$ from the real matrix R such that its dimensions will be $p \times (p+1)/2$ according to:

$$\overline{r_{l,m}} = r_{i,j} + j \quad r_{i,j+1}, 0 \le i \le p, 0 \le j \le p \tag{6}$$

where, $\overline{r_{l,m}}$ refers to the elements of the matrix $\overline{R}$, while $r_{i,j}$ refers to the elements of the matrix R. Matrixes R and $\overline{R}$ are given by:

$$\mathcal{R} = \begin{bmatrix} r_{1,1} & r_{1,2} & r_{1,3} \cdots\cdots & r_{1,p+1} \\ r_{2,1} & r_{2,2} & r_{2,3} \cdots\cdots & r_{2,p+1} \\ \vdots & \vdots & \vdots \;\cdots\cdots & \vdots \\ \vdots & \vdots & \vdots \;\cdots\cdots & \vdots \\ r_{p-1,1} & r_{p-1,2} & \cdots\cdots & r_{p-1,p+1} \\ r_{p,1} & r_{p,2} & r_{p,3} \cdots\cdots & r_{p,p+1} \end{bmatrix} \tag{7}$$

$$\overline{\mathcal{R}} = \begin{bmatrix} r_{1,1}+jr_{1,2} & r_{1,3}+jr_{1,4} \cdots\cdots & r_{1,p}+jr_{1,p+1} \\ r_{2,1}+jr_{2,2} & r_{2,3}+jr_{2,4} \cdots\cdots & r_{2,p}+jr_{2,p+1} \\ \vdots \;\vdots & \vdots \;\cdots\cdots \;\vdots & \vdots \\ \vdots \;\vdots & \vdots \;\cdots\cdots \;\vdots & \vdots \\ r_{p-1,1}+jr_{p-1,2} & \cdots\cdots & r_{p-1,p}+jr_{p-1,p+1} \\ r_{p,1}+jr_{p,2} & \cdots\cdots & r_{p,p}+jr_{p,p+1} \end{bmatrix} \tag{8}$$

Complex matrix construction is made for a purpose of increasing bit per Hertz of mapping before resizing mapped data.

Step 7: resize the matrix $\overline{R}$ to a one dimensional vector $r(k)$ of length $p \times (p+1)/2$.

$$r(k) = \left(r_0 \; r_1 \; r_2 \; \ldots\ldots \; r_{p(p+1)/2}\right)^T \tag{9}$$

Step 8: take the 1D-IFFT for the vector, $r(k)$ to obtain the sub-channel modulation.

$$s(k) = \frac{1}{p(p+1)/2} \sum_{k=0}^{N_c - 1} r(k)\, e^{\frac{j 2 \pi k n}{p(p+1)/2}} \tag{10}$$

where N_c number of carriers.

Step 9: finally, convert the vector $s(k)$ to serial data symbols: s_0, s_1, s_2, ... ,s_n .

3. Fast Discrete Wavelet Transform Computation

If we regard the wavelet transform as a filter bank then we can consider wavelet transforming a signal, as passing it through this filter bank. The outputs at different filter stages are the wavelet and scaling function transform coefficients, this is known as sub-band coding.

The following two equations state that the wavelet and scaling function coefficients on a certain scale can be found by calculating a weighted sum of the scaling function coefficients from the previous scale [5, 8].

$$a_j(k) = \sum_m h(m-2k)\, a_{j+1}(m) \tag{11}$$

$$b_j(k) = \sum_m g(m-2k)\, b_{j+1}(m) \tag{12}$$

This means that equations 11 and 12 together form one stage of an iterated digital filter bank and it is referred to the coefficients *h(k)* as the scaling filter and to the coefficients *g(k)* as the wavelet filter. It is shown that the orthogonality requires that the wavelet coefficients are related to the scaling function coefficients by [5]: $g(k) = (-1)^k h(1-k)$, for a finite even length-*n h(k)*.

$$g(k) = (-1)^k h(n-1-k) \tag{13}$$

In wavelet analysis we often speak of approximations and details. The approximations are the high-scale low-frequency components of the signal and the details are the low-scale high-frequency components [9, 16]. The implementation of equations 11 and 12 is illustrated in Figure 2. In this figure two levels of decomposition are depicted, *h* and *g* are low-pass and high-pass filters corresponding to the coefficients *h(k)* and *g(k)* respectively. The down-pointing arrows denote a decimation or down-sampling by two. This splitting, filtering and decimation can be repeated on the scaling coefficients to give the two-scale structure.

The first stage of two banks divides the spectrum of $a_{j+1,k}$ into a low-pass and high-pass band, resulting in the scaling coefficients and wavelet coefficients at lower scale $a_{j,k}$ and $b_{j,k}$. The second stage then divides the low-pass band into another lower low-pass band and a band-pass band.

If the number of coefficients is two, then for computing FDWT consider the following transformation matrix:

$$T_r = \begin{bmatrix} h(0) & h(1) & 0 & 0 & \cdots & \cdots & & \\ 0 & 0 & h(0) & h(1) & \cdots & \cdots & & \\ \vdots & \vdots & \vdots & \vdots & \cdots & \cdots & & \\ 0 & 0 & 0 & 0 & \cdots & \cdots & h(0) & h(1) \\ g(0) & g(1) & 0 & 0 & \cdots & \cdots & & \\ 0 & 0 & g(0) & g(1) & \cdots & \cdots & \vdots & \vdots \\ \vdots & \vdots & \vdots & \vdots & \cdots & \cdots & & \\ 0 & 0 & 0 & 0 & \cdots & \cdots & g(0) & g(1) \end{bmatrix} \tag{14}$$

Here the blank entries are zero, and if the number of coefficients is four, then for computing FDWT consider the following transformation matrix:

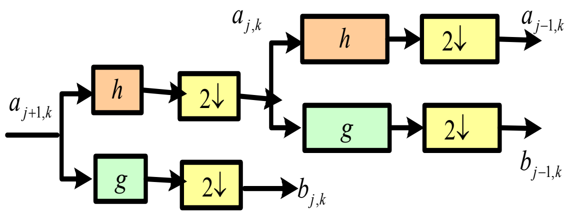

Figure 2. The filter bank for calculating the wavelet coefficients.

$$T_r = \begin{bmatrix} h(0) & h(1) & h(2) & h(3) & 0 & 0 & \cdots & 0 & 0 & 0 & 0 \\ 0 & 0 & h(0) & h(1) & h(2) & h(3) & \cdots & 0 & 0 & 0 & 0 \\ \vdots & \vdots & \vdots & \vdots & \vdots & \vdots & \cdots & \vdots & \vdots & \vdots & \vdots \\ h(2) & h(3) & 0 & 0 & 0 & 0 & \cdots & 0 & 0 & h(0) & h(1) \\ g(0) & g(1) & g(2) & g(3) & \vdots & \vdots & \cdots & 0 & 0 & 0 & 0 \\ 0 & 0 & g(0) & g(1) & g(2) & g(3) & \cdots & 0 & 0 & 0 & 0 \\ \vdots & \vdots & \vdots & \vdots & \vdots & \vdots & \cdots & \vdots & \vdots & \vdots & \vdots \\ 0 & 0 & 0 & 0 & 0 & 0 & \cdots & g(0) & g(1) & g(2) & g(3) \\ g(2) & g(3) & 0 & 0 & 0 & 0 & \cdots & 0 & 0 & g(0) & g(1) \end{bmatrix} \tag{15}$$

By examining the transformation matrices of the scalar wavelet as shown in equations 14 and 15 respectively, it can be seen that the first row generates one component of the data convolved with the low-pass filter coefficients *{h(0), h(1), ...}*. Likewise the second, third, and other upper half rows are formed. The lower half rows perform a different convolution, with high pass filter coefficients *{g(0),g(1), ...}*. The overall action of the matrix is to perform two related convolutions, then to decimate each of them by half (throw away half the values), and interleave the remaining halves. By using equation 13 the transformation matrices becomes:

$$T_r = \begin{bmatrix} h(0) & h(1) & 0 & 0 & \cdots & \cdots & & \\ 0 & 0 & h(0) & h(1) & \cdots & \cdots & & \\ \vdots & \vdots & \vdots & \vdots & \cdots & \cdots & & \\ 0 & 0 & 0 & 0 & \cdots & \cdots & h(0) & h(1) \\ h(1) & -h(0) & 0 & 0 & \cdots & \cdots & & \\ 0 & 0 & h(1) & -h(0) & \cdots & \cdots & \vdots & \vdots \\ \vdots & \vdots & \vdots & \vdots & \cdots & \cdots & & \\ 0 & 0 & 0 & 0 & \cdots & \cdots & h(1) & -h(0) \end{bmatrix} \tag{16}$$

$$T_r = \begin{bmatrix} h(0) & h(1) & h(2) & h(3) & 0 & 0 & \cdots & 0 & 0 & 0 & 0 \\ 0 & 0 & h(0) & h(1) & h(2) & h(3) & \cdots & 0 & 0 & 0 & 0 \\ \vdots & \vdots & \vdots & \vdots & \vdots & \vdots & \cdots & \vdots & \vdots & \vdots & \vdots \\ h(2) & h(3) & 0 & 0 & 0 & 0 & \cdots & 0 & 0 & h(0) & h(1) \\ h(3) & -h(2) & h(1) & -h(0) & \vdots & \vdots & \cdots & 0 & 0 & 0 & 0 \\ 0 & 0 & h(3) & -h(2) & h(1) & -h(0) & \cdots & 0 & 0 & 0 & 0 \\ \vdots & \vdots & \vdots & \vdots & \vdots & \vdots & \cdots & \vdots & \vdots & \vdots & \vdots \\ 0 & 0 & 0 & 0 & 0 & 0 & \cdots & h(3) & -h(2) & h(1) & -h(0) \\ h(1) & -h(0) & 0 & 0 & 0 & 0 & \cdots & 0 & 0 & h(3) & -h(2) \end{bmatrix} \tag{17}$$

It is useful to think of the filter *{h(0),h(1),h(2),h(3)...}* as being a smoothing filter *H*, which something like a moving average of four points. While because of the minus signs, the filter *G={h(3),-h(2),h(1),-h(0),...},* is not a smoothing filter. For such characterization to be useful, it must be possible to reconstruct the original data vector of length *N* from its *N/2* smooth and its *N/2* detail [18]. The requirement of the matrices to be orthogonal leads to that its inverse is just the transposed matrix:

$$T_i = \begin{bmatrix} h(0) & 0 & \cdots & 0 & h(1) & 0 & \cdots & 0 \\ h(1) & 0 & \cdots & 0 & -h(0) & 0 & \cdots & 0 \\ 0 & h(0) & \cdots & 0 & 0 & h(1) & \cdots & 0 \\ 0 & h(1) & \cdots & 0 & 0 & -h(0) & \cdots & 0 \\ 0 & 0 & \cdots & 0 & \cdots & \cdots & \cdots & 0 \\ \vdots & \vdots & \vdots & \vdots & \cdots & \cdots & \vdots & \vdots \\ 0 & 0 & 0 & h(0) & 0 & 0 & 0 & h(1) \\ 0 & 0 & 0 & h(1) & 0 & 0 & 0 & -h(0) \end{bmatrix} \tag{18}$$

$$T_i = \begin{bmatrix} h(0) & 0 & 0 & \cdots & \cdots & h(2) & h(3) & 0 & 0 & \cdots & 0 & h(1) \\ h(1) & 0 & 0 & \cdots & \cdots & h(3) & -h(2) & 0 & 0 & \cdots & 0 & -h(0) \\ h(2) & h(0) & 0 & \cdots & \cdots & 0 & h(1) & h(3) & 0 & \cdots & 0 & 0 \\ h(3) & h(1) & 0 & \cdots & \cdots & 0 & -h(0) & -h(2) & 0 & \cdots & 0 & 0 \\ 0 & h(2) & h(0) & \cdots & \cdots & 0 & 0 & h(1) & h(3) & \cdots & 0 & 0 \\ 0 & h(3) & h(1) & \cdots & \cdots & 0 & 0 & -h(0) & -h(2) & \cdots & 0 & 0 \\ 0 & 0 & h(2) & \cdots & \cdots & 0 & 0 & 0 & h(1) & \cdots & 0 & 0 \\ 0 & 0 & h(3) & \cdots & \cdots & 0 & 0 & 0 & -h(0) & \cdots & 0 & 0 \\ \vdots & \vdots & \vdots & \vdots & \vdots & \vdots & \vdots & \vdots & \vdots & \vdots & \vdots & \vdots \\ & & & 0 & & & & & & & 0 & 0 \\ & & & 0 & h(0) & & & & & & h(3) & 0 \\ & & & 0 & h(1) & & & & & & -h(2) & 0 \\ 0 & 0 & 0 & 0 & h(2) & h(0) & & & & & h(1) & h(3) \\ 0 & 0 & 0 & 0 & h(3) & h(1) & & & & & -h(0) & -h(2) \end{bmatrix} \tag{19}$$

For a length 2 $h(k)$, there are no degrees of freedom left after satisfying the required conditions. These requirements are [5]:

$$\left.\begin{aligned} h(0) + h(1) &= \sqrt{2} \\ h^2(0) + h^2(1) &= 1 \end{aligned}\right\} \tag{20}$$

which are uniquely satisfied by :

$$h_{D2} = \{h(0), h(1)\} = \left\{ \frac{1}{\sqrt{2}}, \frac{1}{\sqrt{2}} \right\} \tag{21}$$

These are the Haar scaling function coefficients, which are also the length 2 Daubechies coefficients. For the length-4 coefficients sequence, there is one degree of freedom or one parameter that gives all the coefficients that satisfy the required conditions:

$$\left.\begin{aligned} h(0) + h(1) + h(2) + h(3) &= \sqrt{2} \\ h^2(0) + h^2(1) + h^2(2) + h^2(3) &= 1 \\ h(0)\, h(2) + h(1)\, h(3) &= 0 \end{aligned}\right\} \tag{22}$$

Letting the parameter be the angle α, the coefficients become

$$\left.\begin{aligned} h(0) &= (1 - \cos\alpha + \sin\alpha)/(2\sqrt{2}) \\ h(1) &= (1 + \cos\alpha + \sin\alpha)/(2\sqrt{2}) \\ h(2) &= (1 + \cos\alpha - \sin\alpha)/(2\sqrt{2}) \\ h(3) &= (1 - \cos\alpha - \sin\alpha)/(2\sqrt{2}) \end{aligned}\right\} \tag{23}$$

These equations give length-2 Haar coefficients for $\pi/2, 3\pi/2$ and length-4 Daubechies coefficients for $\alpha = \pi/3$. These daubechies-4 coefficients have a particularly clean form:

$$h_{D4} = \left\{ \frac{1+\sqrt{3}}{4\sqrt{2}}, \frac{3+\sqrt{3}}{4\sqrt{2}}, \frac{3-\sqrt{3}}{4\sqrt{2}}, \frac{1-\sqrt{3}}{4\sqrt{2}} \right\} \qquad (24)$$

To compute a single level FDWT for 1-D signal the next steps should be followed:

a. Input vector should be of length N, where N must be power of two.
b. Construct a transformation matrix: using transformation matrices given in equations 14 and 15, Transformation of input vector, which can be done by applying matrix multiplication to the NxN constructed transformation matrix by the N*1 input vector. For example let us take a general 1-D signal X. $X = [x_0 \; x_1 \; x_2 \; x_3 \; x_4 \; x_5 \; x_6 \; x_7]$, for an 8x1 input 1-D signal, X construct a 8×8 transformation matrix, T_r, using Haar coefficients filter:

$$T_r = \begin{bmatrix} h(0) & h(1) & 0 & 0 & 0 & 0 & 0 & 0 \\ 0 & 0 & h(0) & h(1) & 0 & 0 & 0 & 0 \\ 0 & 0 & 0 & 0 & h(0) & h(1) & 0 & 0 \\ 0 & 0 & 0 & 0 & 0 & 0 & h(0) & h(1) \\ h(1) & -h(0) & 0 & 0 & 0 & 0 & 0 & 0 \\ 0 & 0 & h(1) & -h(0) & 0 & 0 & 0 & 0 \\ 0 & 0 & 0 & 0 & h(1) & -h(0) & 0 & 0 \\ 0 & 0 & 0 & 0 & 0 & 0 & h(1) & -h(0) \end{bmatrix} \qquad (25)$$

or using Db4 coefficients filter:

$$T_r = \begin{bmatrix} h(0) & h(1) & h(2) & h(3) & 0 & 0 & 0 & 0 \\ 0 & 0 & h(0) & h(1) & h(2) & h(3) & 0 & 0 \\ 0 & 0 & 0 & 0 & h(0) & h(1) & h(2) & h(3) \\ h(2) & h(3) & 0 & 0 & 0 & 0 & h(0) & h(1) \\ h(3) & -h(2) & h(1) & -h(0) & 0 & 0 & 0 & 0 \\ 0 & 0 & h(3) & -h(2) & h(1) & -h(0) & 0 & 0 \\ 0 & 0 & 0 & 0 & h(3) & -h(2) & h(1) & -h(0) \\ h(1) & -h(0) & 0 & 0 & 0 & 0 & h(3) & -h(2) \end{bmatrix} \qquad (26)$$

Transformation of input vector is done as follows: $[Z]_{N*1} = [Tr]_{N*N} \times [X]_{N*1}$. To reconstruct the original signal from the Discrete Wavelet Transformed (DWT) signal, Inverse Fast Discrete Wavelet Transform (IFDWT) should be used. The inverse transformation matrix is the transpose of the transformation matrix as the transform is orthogonal. To compute a single level IFDWT for 1-D signal the next steps should be followed:

a. Let X be the Nx1 wavelet transformed vector.
b. Construct NxN reconstruction matrix, T_i, using transformation matrices given in equations 18 and 19.
c. Reconstruction of input vector, which can be done by applying matrix multiplication to the NxN reconstruction matrix, T_i, by the Nx1 wavelet transformed vector. For example, let X be the input 1-D signal, $X = [x_0 \; x_1 \; x_2 \; x_3 \; x_4 \; x_5 \; x_6 \; x_7]$, for an 8×1 input 1-D signal, X, construct a 8×8 reconstruction matrix, T_i, using Haar coefficients filter:

$$T_i = \begin{bmatrix} h(0) & 0 & 0 & 0 & h(1) & 0 & 0 & 0 \\ h(1) & 0 & 0 & 0 & -h(0) & 0 & 0 & 0 \\ 0 & h(0) & 0 & 0 & 0 & h(1) & 0 & 0 \\ 0 & h(1) & 0 & 0 & 0 & -h(0) & 0 & 0 \\ 0 & 0 & h(0) & 0 & 0 & 0 & h(1) & 0 \\ 0 & 0 & h(1) & 0 & 0 & 0 & -h(0) & 0 \\ 0 & 0 & 0 & h(0) & 0 & 0 & 0 & h(1) \\ 0 & 0 & 0 & h(1) & 0 & 0 & 0 & -h(0) \end{bmatrix} \qquad (27)$$

or using Db4 coefficients filter:

$$T_i = \begin{bmatrix} h(0) & 0 & 0 & h(2) & h(3) & 0 & 0 & h(1) \\ h(1) & 0 & 0 & h(3) & -h(2) & 0 & 0 & -h(0) \\ h(2) & h(0) & 0 & 0 & h(1) & h(3) & 0 & 0 \\ h(3) & h(1) & 0 & 0 & -h(0) & -h(2) & 0 & 0 \\ 0 & h(2) & h(0) & 0 & 0 & h(1) & h(3) & 0 \\ 0 & h(3) & h(1) & 0 & 0 & -h(0) & -h(2) & 0 \\ 0 & 0 & h(2) & h(0) & 0 & 0 & h(1) & h(3) \\ 0 & 0 & h(3) & h(1) & 0 & 0 & -h(0) & -h(2) \end{bmatrix} \qquad (28)$$

Reconstruction of input vector can be done as follows: $[Z]_{N*1} = [Ti]_{NxN} \times [X]_{N*1}$

4. Proposed System for Radon-Wavelet Based OFDM Transceiver

Due to good orthogonality of both DWT and FRAT which reduce ISI and ICI, in proposed system there is no need of using Cyclic Prefix (CP). The block diagram of the proposed Radon-wavelet based OFDM system is depicted in Figure 3 and the IDWT modulator and DWT demodulator are shown in Figure 4.

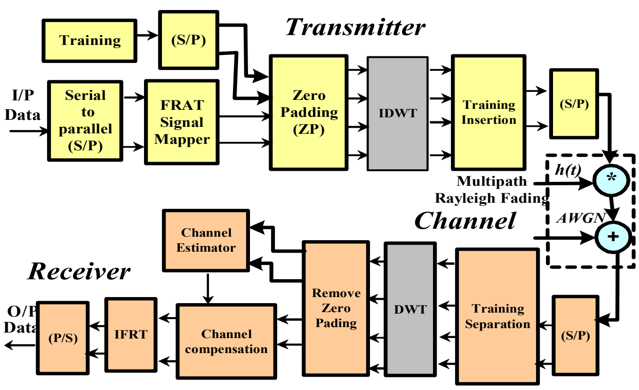

Figure 3. Block diagram of FRAT-DWT based OFDM system.

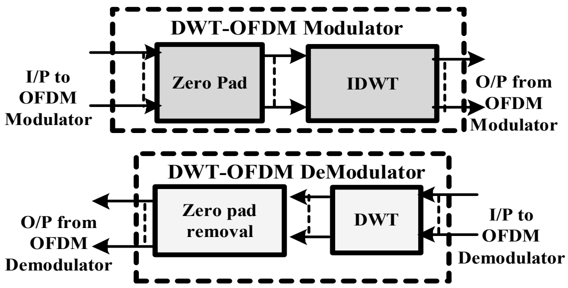

Figure 4. DWT-OFDM modulation- demodulation.

The processes of Serial to Parallel (S/P) converter, signal demapper, and the insertion of training sequence are the same as in the system of FFT-OFDM. Also the zeros are added as in the FFT based case and for the same reasons. After that the IDWT is applied to the signal. The main and important difference between FFT based OFDM and DWT based OFDM is that in wavelet based OFDM cyclic prefix is not added to OFDM symbols. Therefore the data rates in wavelet based OFDM is higher than those of the FFT based OFDM. At the receiver, the zeros padded at the transmitter are removed, and the other operations of channel estimation, channel compensation, signal demapping and Parallel to Serial (P/S) are performed in the same manner as in FFT based OFDM..

In conventional OFDM system, the length of input data frame is 60 symbols, and after (S/P) conversion and QAM mapping the length becomes 30 symbols. Zero padding operation makes the length 64 symbols which are the input to IFFT (sub-carrier modulation). After adding CP (usually 40% of the length of the frame), the frame length becomes 90 symbols. Since OFDM operations applied to training symbols are the same as those applied to transmitted data (except the mapping operation), the length of training symbols is also 90 symbols. The training and data frames are transmitted as one frame starting with training, so the length of transmitted frame is 180 symbols [22]. In proposed system, the length of the input data frame must be *(pxp),* where *P* is a prime number. The closest number to 60 is 7x7, which makes the frame length 49 symbols. This is because the input of FRAT must be a two dimensional matrix with size *(pxp*).

5. Simulation Results of the Proposed System

Four types of OFDM systems were simulated: FFT-OFDM, Radon-OFDM, DWT-OFDM and proposed Radon-DWT based OFDM systems using MATLAB version 7. The BER performances of the four systems were found for different channel models: AWGN channel, flat fading channel, and selective fading channel. System parameters used through the simulations are: $T_S = 0.1\mu\text{sec}$, FRAT window: 7 by 7, and DWT bins $N = 64$.

5.1. Performance of Proposed OFDM System in AWGN channel

Figure 5 shows the results of simulation of proposed system compared with other systems in AWGN channel. It is clearly seen that FRAT-DWT based OFDM has better performance than the other three systems: FFT-OFDM, DWT-OFDM and FRAT-OFDM. This is due to the high orthogonality of proposed system. To have BER = 10^{-4}, FFT-OFDM requires 28 dB, FRAT-OFDM requires 25 dB, DWT-OFDM requires 21.5 dB, and FRAT-DWT based OFDM requires 17 dB. And to have BER = 10^{-5}, FFT-OFDM requires 31.5 dB, FRAT-OFDM requires 28 dB, DWT-OFDM requires 23.5 dB, and FRAT-DWT based OFDM requires 18.5 dB. From the results it can be noted that proposed system has 12 dB advantage over FFT-OFDM, 9.5 dB over FRAT-OFDM, and 5 dB over DWT-OFDM.

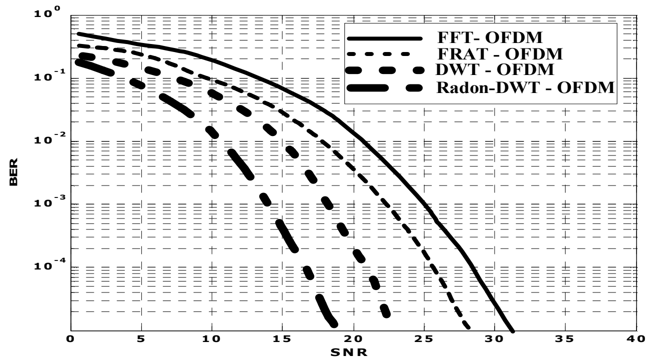

Figure 5. BER performance of FRAT-DWT based OFDM in AWGN channel.

5.2. Performance of the Proposed OFDM System in Flat Fading Channel with AWGN

In this channel, all signal frequency components are affected by a constant attenuation and linear phase distortion, in addition to an AWGN. The channel was selected to be multi-path and Rayleigh distributed. Doppler frequency used in simulation is calculated as follows: $c = 300\times10^6 m/\text{sec}$, in GSM system $f_c = 900\,MHz$ so,

$$f_d = f_c \times \frac{v}{c} = 900 \times 10^6 \times \frac{1}{\text{sec}} \times \frac{v}{300 \times 10^8\ m/\text{sec}}$$

$$f_d = 3/(1m) \times v$$

The Doppler frequency used, is that corresponding to a walking speed (4.8 km/hour), and it has a value: $f_d = \frac{3}{1m} \times \frac{4.8 \times 1000\ \ m}{3600\ \ \text{sec}} = 4\,Hz$, The results of simulations for 4Hz Doppler frequency are shown in Figure 6. From Figure 6 it can be seen that to have BER = 10^{-5}, FFT-OFDM requires 33dB, FRAT-OFDM requires 30.5dB, DWT-OFDM requires 25dB, and FRAT-DWT based OFDM requires 20.5dB. So proposed system offers 12.5 dB SNR-improvement compared with FFT-OFDM, 10 dB compared with FRAT-OFDM, and 4.5dB compared with DWT-OFDM for this channel model. Other Doppler-Shift frequencies were used for proposed system simulation over the flat fading Rayleigh channel; the values used are 80Hz corresponding to car speed (96 km/hour), 300Hz corresponding to Helicopter speed (360 km/hour), and 500Hz corresponding to airplane speed (600 km/hour), and the same results were obtained for these frequencies. The reason for best performance results of FRAT-DWT based OFDM is the good orthogonality of Radon transform and the excellent orthogonality of DWT.

5.3. BER Performance of the Proposed OFDM System in Selective Fading Channel with AWGN

In this section, the channel model is assumed to be selective fading channel. A second ray's Raleigh-distributed multi-path fading channel is assumed, where the parameters of the multipaths channel are: path gain equal -8 dB and path delay $\tau_{\max} = 0.1\mu\sec$.

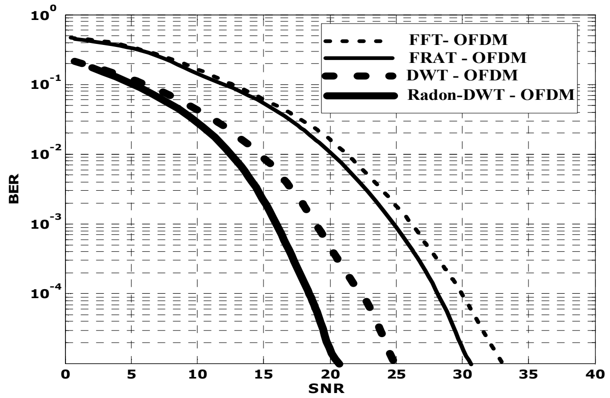

Figure 6. BER performance of FRAT-DWT based OFDM in flat fading channel at Doppler frequency 4 Hz.

The BER performance of proposed system and the other OFDM systems over a selective fading channel with Doppler frequency of 4 Hz is shown in Figure 7. It can be seen that to have BER = 10^{-5}, FFT-OFDM requires 37.5 dB, FRAT-OFDM requires 34.5 dB, DWT-OFDM requires 28 dB, and FRAT-DWT based OFDM requires 22 dB. So proposed system offers a large SNR-improvement compared with FFT-OFDM, FRAT-OFDM, and DWT-OFDM for this channel model.

The same performance characteristics of systems over selective fading channel with Doppler frequencies 80 Hz, 300 Hz, and 500 Hz were simulated. Figure 8 shows BER performance of FRAT-DWT based OFDM in selective fading channel with Doppler frequency of 300 Hz. From Figure 8, it is clearly seen that FFT based OFDM needs more than 40 dB of SNR to have BER= 10^{-4}, while FRAT based OFDM needs around 39 dB of SNR to reach BER=10^{-5}, DWT based OFDM BER performance does not exceed 0.002425 with increasing SNR, whereas proposed FRAT-DWT based OFDM has much better performance than the other three systems, it reaches BER=10^{-5} at SNR= 26.5 dB.

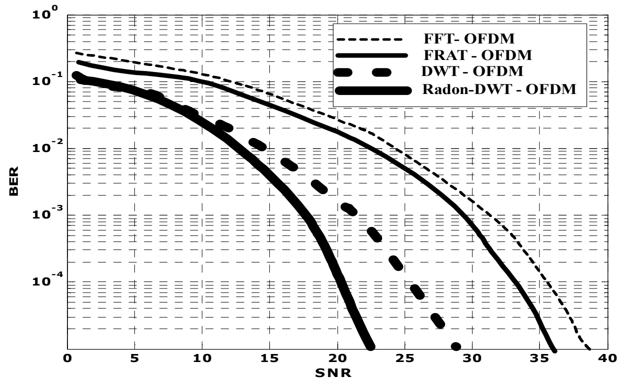

Figure 7. BER performance of FRAT-DWT based OFDM in selective Fading Channel at Doppler frequency 4 Hz.

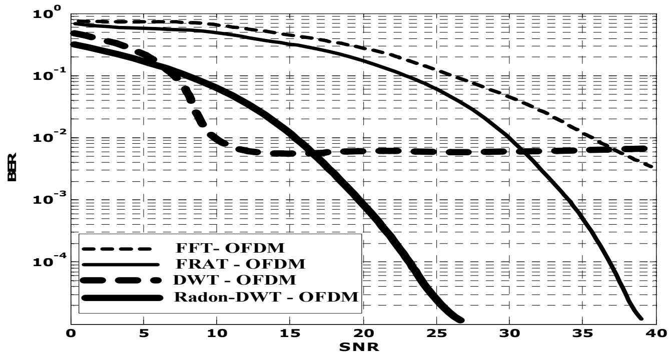

Figure 8. BER performance of FRAT-DWT based OFDM in selective fading channel at Doppler frequency 300 Hz.

Figure 9 shows BER performance of FRAT-DWT based OFDM in selective Fading Channel with Doppler frequency of 500Hz. From Figure 9, the following conclusion can be stated: When Doppler frequency exceeds 500 Hz, proposed system suffers from the same problem that DWT based OFDM system suffer from, the performance of proposed system does not increase with increasing SNR when the Doppler frequency exceed 500 Hz. It is seen that OFDM systems are very sensitive systems to the variation of Doppler frequency in selective fading channel.

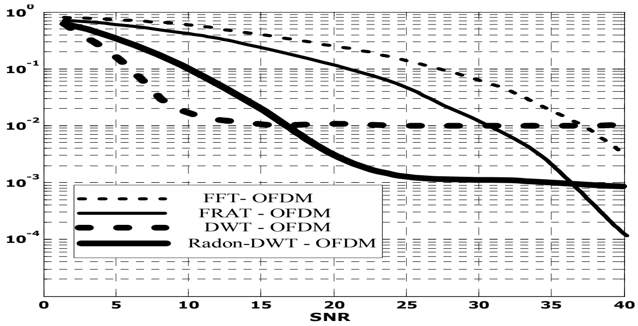

Figure 9. BER performance of FRAT-DWT based OFDM in selective fading channel at Doppler frequency 500 Hz.

The effect of Doppler frequency value on BER performance for proposed system is provided in Figure 10. It can be seen from Figure 10 that the critical value of Doppler frequency for proposed system is around 420 Hz.

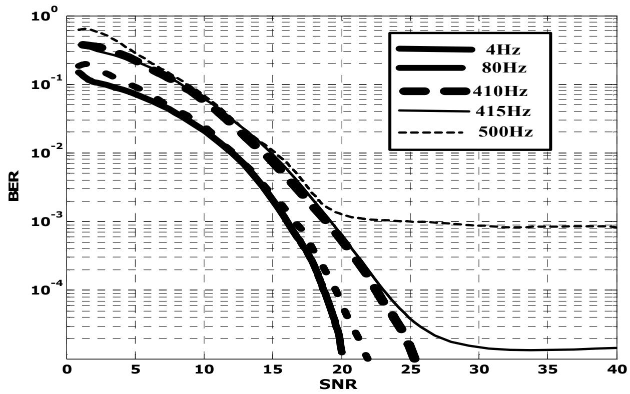

Figure 10. BER performance of FRAT-DWT based OFDM in selective fading channel at different Doppler frequencies.

6. Conclusions

In this paper a novel OFDM generation method is proposed, simulated, and tested. The proposed system uses Radon-DWT mapping instead of QAM mapping which increases the orthogonality. The optimal ordering (best direction) in the Radon mapper can be considered as a good interleaver which serve in error spreading. In proposed system there is no need for using CP because of excellent orthogonality offered by FRAT and DWT, which in its order reduces the system complexity, increases the transmission rate, and increases spectral efficiency. Simulation results of proposed Radon-DWT based OFDM show a very good SNR gain improvement and a BER performance as compared with DWT-OFDM, FRAT-OFDM, and FFT-OFDM in an AWGN, a flat fading, and a selective fading channels. It offers more than 15 dB SNR improvement compared with FFT-OFDM for selective Fading Channel at Doppler frequency 4Hz. From the simulation results, it can be seen that proposed Radon-DWT based OFDM has the smallest sensitivity to variations of the channel parameters. This work will be continued towards designing a Radon-DWT multi-carrier code division multiple access system with an increased SNR improvement under severe channel conditions.

References

[1] Al-Dhahir N. and Cioffi J., "Optimum Finite-Length Equalization for Multicarrier Transceivers," *Computer Journal of IEEE Transactions Communications*, vol. 44, no. 1, pp. 56-64, 1996.

[2] Al-Jawhar W., Kattoush A., Abbas S., and Shaheen A., "A High Speed High Performance Parallel Radon Based OFDM Transceiver Design and Simulation," *Computer Journal of Digital Signal Processing*, vol. 18, no. 11, pp. 907-918, 2008.

[3] Beylkin G., "Discrete Radon Transforms," *Computer Journal of IEEE Transactions Acoustic, Speech, and Signal Processing*, vol. 35, no. 2, pp. 162-172, 1987.

[4] Bolker D., "The Finite Radon Transform," *Integral Geometry and Contemporary Mathematics*, vol. 63, no. 2, pp. 27-50, 1987.

[5] Burrus S., Gopinath R., and Guo H., *Introduction to Wavelets and Wavelet Transforms: A Primer*, Prentice Hall, 1998.

[6] Cimini L., "Analysis and Simulation of a Digital Mobile Channel Using Orthogonal Frequency Division Multiplexing," *Computer Journal of IEEE Transactions on Communication*, vol. 33, no. 3, pp. 665-675, 1985.

[7] Deans R., *The Radon Transform and Some of its Applications*, John Wiley and Sons, 1983.

[8] Graps A., "An Introduction to Wavelets," *Computer Journal of IEEE Computational Science and Engineering*, vol. 2, no. 2, pp. 50-61, 1995.

[9] Goswami C. and Chan K., *Fundamentals of Wavelets Theory, Algorithms, and Applications*, John Wiley and Sons Ltd, 1999.

[10] *IEEE Std., IEEE Proposal for 802.16.3, RM Wavelet Based PHY Proposal for 802.16.3*, Rainmaker Technologies, 2001.

[11] Koffman I. and Roman V., "Broadband Wireless Access Solutions Based on OFDM Access in IEEE 802.16," *IEEE Communication Magazine*, vol. 40, no. 4, pp. 96-103, 2002.

[12] Lawrey E., "The Suitability of OFDM as a Modulation Technique for Wireless Telecommunications, with a CDMA Comparison," *Thesis* James Cook University, 1997.

[13] Lee I., Chow J., and Cioffi J., "Performance Evaluation of a Fast Computation Algorithm for the DMT in High-Speed Subscriber Loop," *Computer Journal of IEEE Select Areas Communication*, vol. 13, no. 9, pp. 1564-1570, 2007.

[14] Lindsey R., "Wavelet Packet Modulation for Orthogonally Multiplexed Communication," *Computer Journal of IEEE Transactions Signal Process*, vol. 45, no. 5, pp. 1336-1337, 1997.

[15] Mallat S., *A Wavelet Tour of Signal Processing*, Academic Press, 1999.

[16] Mallat S., "A Theory for Multiresolution Signal Decomposition: the Wavelet Representation," *Computer Journal of IEEE Pattern Analysis and Machine Intelligence,* vol. 11, no. 7, pp. 674-693, 1989.

[17] Minh N. and Martin V., "The Finite Ridgelet Transform for Image Representation," *Computer Journal of IEEE Transactions Image Processing*, vol. 12, no. 1, pp. 16-28, 2003.
[18] Mohammed J., "VIDEO Image Compression Based on Multiwavelets Transform," *PhD Thesis*, University of Baghdad, 2004.
[19] Nee V. and Prasad R., *OFDM for Wireless Multimedia Communications*, Artech House, 2000.
[20] Nghi H., Ha H., and Le-Ngoc T., "Bit-Interleaved Coded OFDM with Signal Space Diversity: Subcarrier Grouping and Rotation Matrix Design," *Computer Journal of IEEE Transactions on Signal Processing*, vol. 55, no. 3, pp. 1137-1149, 2007.
[21] Prasad R., *OFDM for Wireless Communications Systems*, Artech House Publishers, 2004.
[22] Proakis G., *Digital Communications*, McGraw Hill, 2001.
[23] Resnikoff L., Raymond J., and Wells O., *Wavelet Analysis, The Scalable Structure of Information*, Springer, 1998.
[24] SeungWon K. and KyungHi C., "A Novel Channel Estimation Scheme for OFDM/OQAM-IOTA System," *Computer Journal of Electronics and Telecommunications Research Institute*, vol. 29, no. 4, pp. 430-436, 2007.
[25] Weinstein S. and Ebert P., "Data Transmission by Frequency Division Multiplexing Using the Discrete Fourier Transform," *Computer Journal of IEEE Transactions Communications* Tech, vol. 19, no. 3, pp. 628-634, 1971.
[26] Won G., Kyung C., and Yong C., "An Equalization Technique for Orthogonal Frequency Division Multiplexing Systems in Time-Variant Multipath Channels," *Computer Journal of IEEE Transactions on Communications*, vol. 47, no. 1, pp. 27-32, 1999.
[27] Zhang X., Xu P., Zhang G., and Bi G., "Study on Complex Wavelet Packet Based OFDM Modulation," *Computer Journal of ACTA Electron*, vol. 30, no. 4, pp. 476-479, 2002.
[28] Zhang H., Yuan D., Jiang M., and Wu D., "Research of DFT-OFDM and DWT-OFDM on Different Transmission Scenarios," *in Proceedings of IEEE ICITA'2004*, China, pp. 125- 127, 2004.
[29] Zhang H., Dongfeng Y., Matthias P., "Novel Study on PAPRs Reduction in Wavelet-Based Multicarrier Modulation Systems," *Computer Journal of Elsevier Digital Signal Processing*, vol. 17, no. 3, pp. 272-279, 2007.

Abbas Kattoush received his MS and PhD degrees in communication engineering from USSR in 1979 and 1984, respectively. For 10 years he was a technical manager of a leading SAKHER computers company. He was a pioneer in computer networking and software engineering in Jordan. From 1993 to 2000 he worked at Applied Science University Amman Jordan where he was a founding member of the Department of Electrical and Computer Engineering. From 2000 to 2008 he was an associate professor at Electrical and Computer Engineering Department at Al-Isra University, Amman-Jordan.